

Supplementary text I: Photogrammetry processing

After surveying the subcatchment in Endalen valley by drone, we process the survey in the photogrammetrical suite Agisoft Metashape version 1.8.4 using the default processing settings. We register the survey data to the 2009 Digital Elevation Model (DEM) made by well-georeferenced aerial images by the Norwegian Polar Institute (Norwegian Polar Institute, 2014), using Iterative Closest Point (ICP) registration in CloudCompare version 2.12, leading to a mean vertical bias of 0.03 m, and a mean absolute point-to-point distance (which we consider the registration uncertainty) of 0.74 m. We assume minimal internal distortion in the survey due to the inclusion of oblique images (James et al., 2017) and therefore consider the affine transformation of the ICP registration sufficient for the accuracy that is required for the study. With a survey diameter of 990 m, this location uncertainty is approximately equivalent to an angle uncertainty of 0.04° ($\tan^{-1} \frac{0.74}{990}$).

Supplementary text II: Carbon distribution in Adventdalen, Svalbard

Slopes in the greater Adventdalen area are generally often characterized by the occurrence of solifluction processes. Solifluction can lead to the burial of organic matter into deeper soil layers, enriching the organic carbon content in samples taken from different tributaries of the Adventdalen valley (such as the Endalen valley). Sampling soil cores in Adventdalen by Weiss et al. (2017) has revealed that SOC 0–100 cm stocks in solifluction affected areas are on average 20.7 kg C m^{-2} , which is much higher than the landscape-level mean of 4.2 kg C m^{-2} based on landform upscaling.

Fig. S1 shows examples of four profiles from two solifluction areas in Adventdalen. The mean SOC 0–100 cm stock of these profiles is 23.4 kg C m^{-2} , slightly higher than the reported mean stock for solifluction areas reported in Weiss et al. (2017). Profiles are generally deep before reaching bedrock or regolith ($\geq 70 \text{ cm}$). They have a thin top organic layer ($\%C < 10$) between 4.5–9 cm (mean 6.4 cm), which stores only 3.0–9.9% (mean 5.5%) of the total SOC stock in the top 100 cm of the profiles. The remainder is stored in the mineral active layer, with negligible amounts in the permafrost layer. Only in profile T3-1, the frost table was reached at 70 cm on the sampling date of July 1, 2013 but the active layer depth is certainly much deeper. Two profiles show some C-enrichment at greater depth, likely the result of burial by solifluction processes (T3-1 at 36–60 cm and T5-8 at 18–30 cm). T5 profiles have a larger volume of large stones in their profiles (up to 50%), which reduces total SOC 0–100 cm stocks compared to T3 profiles (no large stones, not shown).

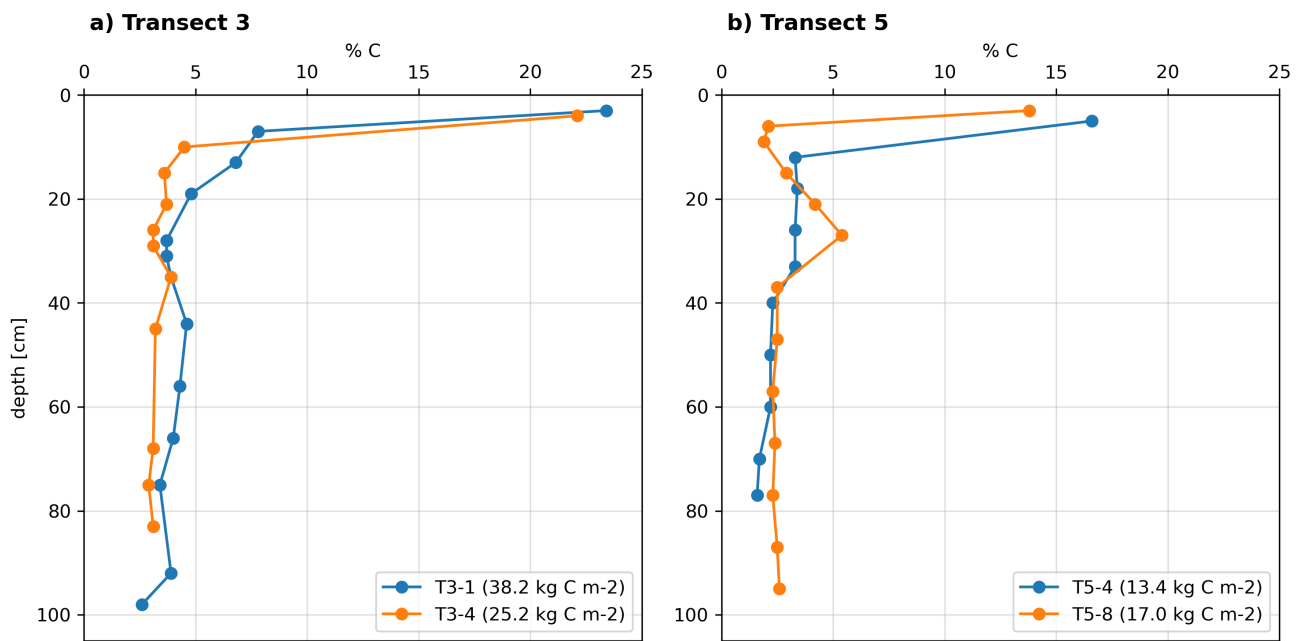


Figure S1: Organic carbon content (%) vs depth (cm) in four examples of soil profiles from the Adventdalen area. Transect 3 (a) is close to the Endalen valley, which represents the study site in this paper. Transect 5 (b) is located close to the Bolterdalen valley, ~6.5 km southeast of the Endalen valley. Sampling depths vary depending on the sampling method and quality of the soil profiles retrieved. The total soil organic carbon storage in each profile is denoted in the legend entry next to the profile ID.

Supplementary figures

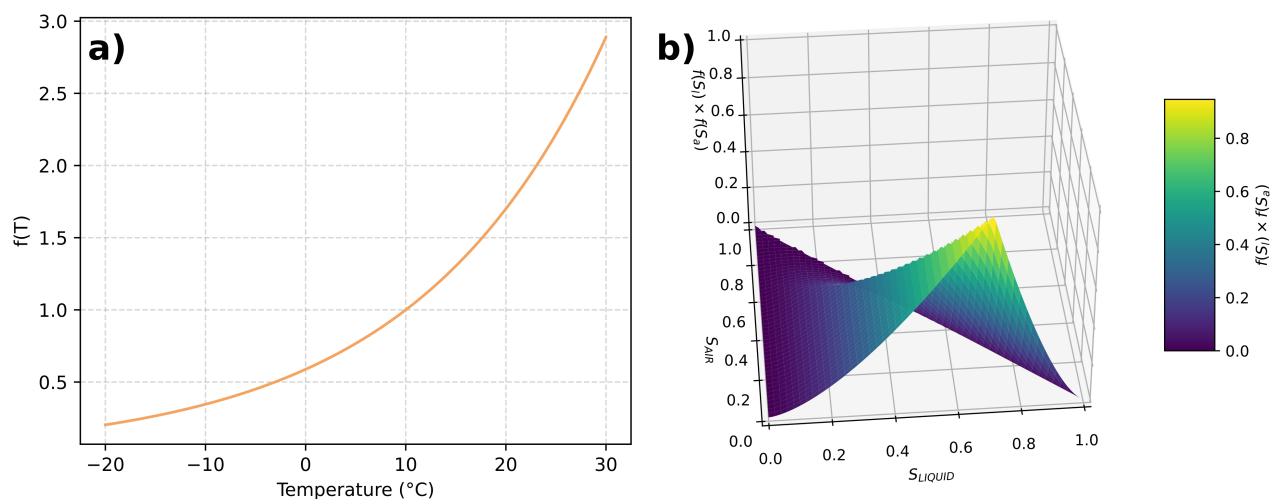


Figure S2: Functions (a) $f(T)$ using Eq. (3) and (b) $f(S_l) \times f(S_a)$ using Eqs. (4) and (5) in the main text, for a temperature range of -20–30 $^{\circ}\text{C}$, and a liquid and gas saturation range of 0–1. The value on the y-axis corresponds to the scaling factor that is then used in Eq. (2) in the main text.

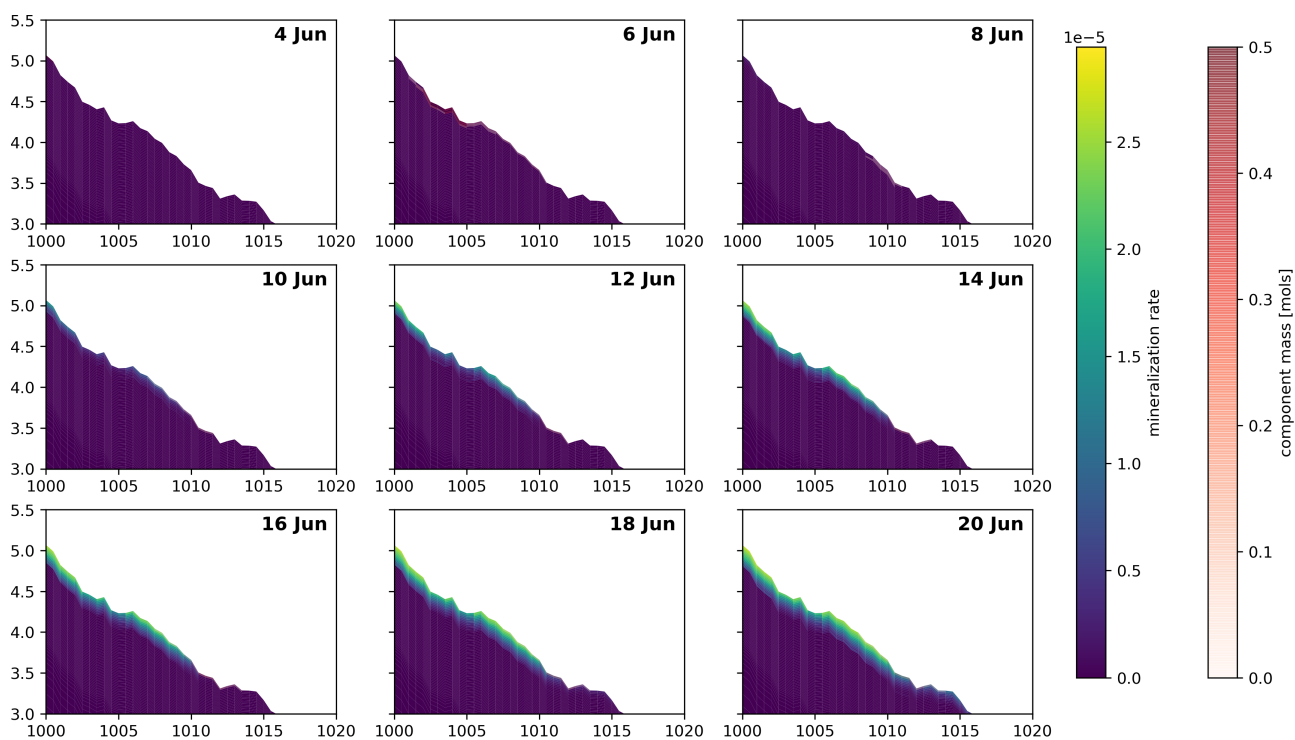


Figure S3: Potential normalized mineralization rate and component mass of TOL carbon throughout the transect for selected dates in the early thawing season similar to Fig. 8 in the main text. Blue areas mark comparably low potential mineralization rates, yellow areas indicate the highest potential for mineralization. Component mass is added as a white to red overlay and is the same as in Fig. 8 in the main text.

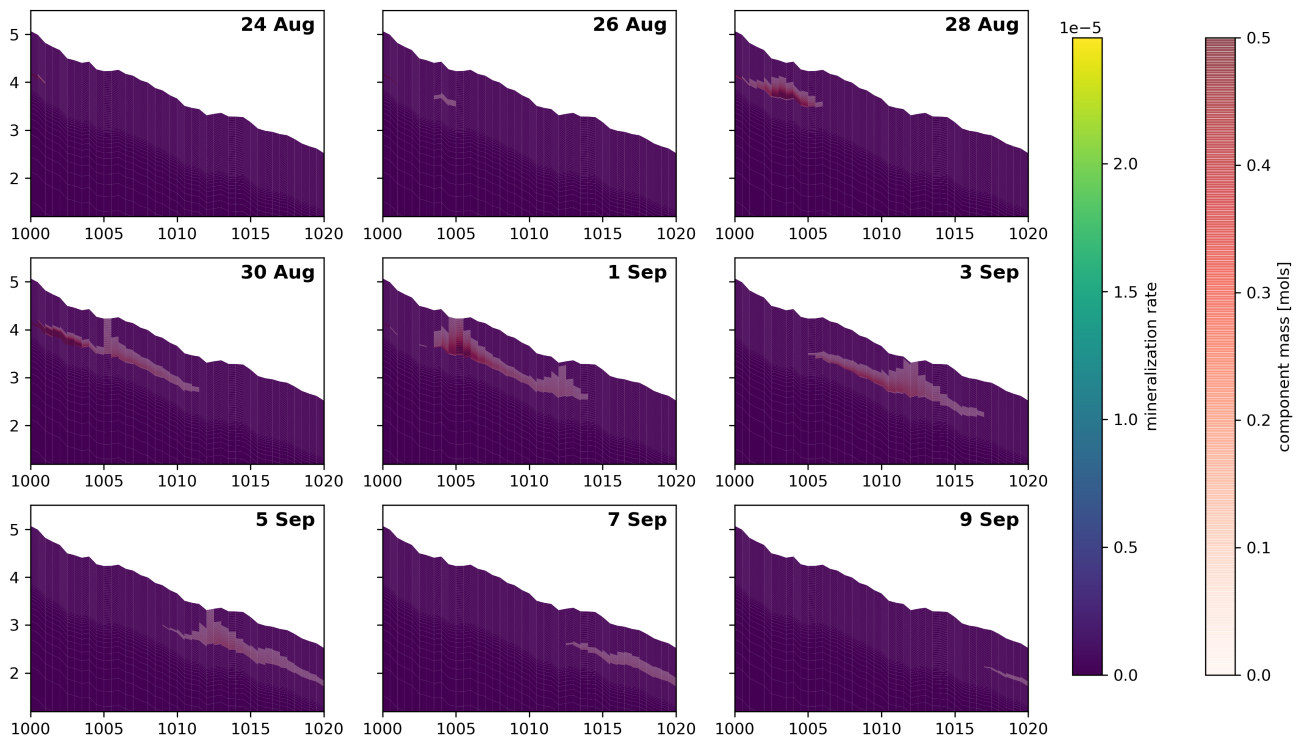


Figure S4: Potential normalized mineralization rate and component mass of buried carbon throughout the transect for selected dates in the early thawing season similar to Fig. 9 in the main text. Blue areas mark comparably low potential mineralization rates, yellow areas indicate the highest potential for mineralization. Component mass is added as a white to red overlay and is the same as in Fig. 9 in the main text.

References

- James, M. R., Robson, S., and Smith, M. W.: 3-D uncertainty-based topographic change detection with structure-from-motion photogrammetry: precision maps for ground control and directly georeferenced surveys: 3-D uncertainty-based change detection for SfM surveys, *Earth Surface Processes and Landforms*, 42, 1769–1788, <https://doi.org/10.1002/esp.4125>, URL <http://doi.wiley.com/10.1002/esp.4125>, 2017.
- 30 Norwegian Polar Institute: Terrengmodell Svalbard (S0 Terrengmodell), <https://doi.org/10.21334/npolar.2014.dce53a47>, URL <https://data.npolar.no/dataset/dce53a47-c726-4845-85c3-a65b46fe2fea>, type: dataset, 2014.
- Weiss, N., Faucherre, S., Lampiris, N., and Wojcik, R.: Elevation-based upscaling of organic carbon stocks in High-Arctic permafrost terrain: a storage and distribution assessment for Spitsbergen, Svalbard, *Polar Research*, 36, 1400 363, <https://doi.org/10.1080/17518369.2017.1400363>, URL <https://polarresearch.net/index.php/polar/article/view/2678>, 2017.